MOLECULAR SIMULATION OF HYDROXYPROPYL-β-CYCLODEXTRIN WITH HYDROPHOBIC SELECTIVE COX-II CHEMOPREVENTIVE AGENT USING HOST-GUEST PHENOMENA

VIVEK RANJAN SINHA[*], AMITA NANDA, RENU CHADHA and HONEY GOEL

University Institute of Pharmaceutical Sciences, Panjab University, Chandigarh 160014, India

Abstract: The present investigation outlays the host-guest penetration of hydrophobic selective Cox-II chemo-preventive agent, celecoxib (CXB), with hydroxypropyl-β-cyclodextrin (HP-β-CD) using inclusion complexa-tion phenomena. Phase solubility studies conducted at 37°C and 25°C revealed typical A_L-type curve for the HP-β-CD indicating the formation of soluble complexes. The inclusion complexes in the molar ratio of 1:1 and 2:1 (CXB-HP-β-CD) were prepared by kneading technique. The formation of inclusion complexes and the molecular simulation of CXB protons with HP-β-CD cavity in all samples were testified by ^{1}H-NMR, DSC, powder-XRD, SEM and FTIR and UV/visible spectroscopy. The results of these studies indicated that complex (prepared by kneading method) in molar ratio of 1:1 exhibited better improvement in *in vitro* dissolution pro-files as compared to 1:2 complex. Mean *in vitro* dissolution time indicated significant difference in the release profiles of CXB from complexes and physical mixtures as compared to pure CXB.

Keywords: celecoxib (CXB), inclusion complexes, hydroxypropyl-β-cyclodextrin (HP-β-CD), dissolution

Cyclodextrins (CDs) have been described as "promising molecules, appealing to investigators in both pure research and applied technologies" (1). The safety profiles of the three most common natu-ral CDs and some of their derivatives have been reviewed (2). All toxicity studies have demonstrated that orally administered CDs are practically non-toxic due to lack of absorption from the gastroin-testinal tract (3). HP-β- CDs were shown to have a better oral safety profile than β-CD and other parent CDs, but only limited data are available on the oral safety of the methylated CDs. CDs may themselves cause cutaneous irritation as they release some com-ponents such as cholesterol, phospholipids and pro-teins from stratum corneum of skin. This may con-sequently change the barrier function of skin and the permeability of drugs or other xenobiotics (4). When poor bioavailability is due to low solubility, CDs are of extreme value. They enhance the bioavailability of insoluble drugs by increasing the drug solubility, dissolution and/or drug permeability (5).

CD complexation is of immense application in improving the chemical, physical and thermal sta-bility of drugs. For an active molecule to degrade upon exposure to oxygen, water, radiation or heat, chemical reactions must take place. When a mole-cule is entrapped within the CD cavity, it is difficult for the reactants to diffuse into the cavity and react with the protected guest (6).

CD derivatives such as amorphous HP-β-CD and sulfobutyl ether (SBE)-β-CDs have been wide-ly investigated for parenteral use on account of their high aqueous solubility and minimal toxicity. HP-β-CD, which has higher aqueous solubility, allows parenteral administration of various drugs with no significant toxicity problems and hence is more often used in parenteral formulations. An itracona-zole parenteral injection containing HP-β-CD (40% w/v) has been commercialized in USA and Europe. CXB was the first, specific cyclooxygenase–II (COX–II) inhibitor approved in US for patients with rheumatoid and osteoarthritis. The conventional non-steroidal anti-inflammatory drugs (NSAIDs) act by inhibiting both cyclooxygenase enzyme I and II. They inhibit the cyclooxygenase–I (COX–I) that is involved in beneficial functions such as gastroin-testinal mucosal protection, platelet function and regulation of renal hemodynamics and electrolyte balance. As a result, their use is associated with an elevated risk of damage to the gastrointestinal mucosa and related complications. CXB produces significant improvements in pain and inflammation without causing gastrointestinal damage.

Recently various clinical trials are under process globally due to significant anti-carcinogenic

* Corresponding author: e-mail: sinha_vr@rediffmail.com

potential of CXB shown in human carcinoma cell lines and various *in vivo* animal models (7–9). This drug has revamped new interest among the researchers to utilize its chemopreventive action against cancerous growth. However, CXB belongs to Class II type drugs according to BCS. It exhibit very poor aqueous solubility (3–7 μg/mL in 40°C at pH 7) and was shown to have dissolution rate limited bioavailability (10).

In this study, the inclusion complex of HP-β-CD with CXB was obtained by widely known kneading technique, for the preparation of inclusion complexes. The objective of the present work was to prepare and characterize the hydrophobic selective COX-II blocker – HP-β-CD complexes and further to investigate the possibility of improving the solubility and dissolution of ETD by complexation with HP-β-CD.

MATERIALS AND METHODS

CXB was a generous gift from Cadila Pharmaceuticals Ltd., (Ahmedabad, India). HP-β–CD was obtained from S.A. Chemicals, (Mumbai, India). All chemicals and solvents used in this study were of analytical grade. Fresh ultrapure water (MILLI-Q) was used throughout the work.

Analytical procedure

Twenty five mg of CXB was carefully weighed into a 50 mL conical flask. Solubility studies were carried by adding excess quantity of CXB (25 mg) in 20 mL of aqueous solution containing CDs at various concentrations (1.0×10^{-3} M – 8.0×10^{-3} M) (11). The flasks were closed and equilibrated by shaking at 25°C and 37°C. When equilibrium was reached (48 h), the samples were filtered through a 0.22 μm membrane filter (Sartorius cellulose nitrate filter, Germany). The filtrates were assayed for drug content by ultraviolet spectroscopy (Shimadzu-1601, USA) at 278 nm. The apparent 1:1 stability constants, K_s, were calculated from the initial straight line portion of the phase solubility diagram according to the following equation (12):

$$K_s = Slope/S_o(1 - Slope) \qquad (1)$$

where S_o is the saturation concentration of drug measured without HP-β-CD.

Preparation of binary inclusion systems

A molar ratio 1:1 (CXBKDHP1) and 1:2 (CXBKDHP2) were used to prepare the complexes by kneading method using CXB and HP-β-CD. Slurry was prepared by wetting CD with water in a mortar until a paste was obtained. CXB was then added in divided proportions and kneaded for 1 h. Appropriate amount of water was added in order to maintain suitable consistency. Further, the product obtained was washed with dichloromethane to remove the uncomplexed drug. Then, the product was dried under vacuum at 40°C for 48 h.

The physical mixtures of CXB and HP-β-CD were prepared by passing the drug and HP-β-CD through mesh #60 separately and then mixing both solids by simple blending. Various molar ratios of CXB and HP-β-CDs were used to prepare physical mixtures 1:1 (CXBPM1) and 1:2 (CXBPM2).

Physicochemical characterization

The complexes were analyzed for physicochemical parameters in solid state as well as solution state. ^{1}H-NMR experiments were performed at 500 MHz using a Bruker AVANCE DPX 300 spectrometer. The probe temperature was regulated at 298 K. CD_3OD and D_2O (1:1 mixture) as solvent system with tetramethylsilane (TMS) as internal standard were used in each case. The conditions for Fourier transform measurements were as follows: acquisition time 5.19 s; pulse angle 30°; delay time 5 s; number of scans used 103. Shift value of the complexes (HP-β-CD bound drug) and free HP-β-CD are recorded under the same conditions and in the same solvent system.

DSC of the complexes and physical mixtures were carried out (Mettler Toledo STAR System, Swizterland) in sealed aluminium (Al) pans before heating under nitrogen flow (20 mL/min) at a scanning rate of 10°C from 0° to 450°C. An empty Al pan was used as a reference. The equipment was periodically calibrated with indium.

The external morphology of inclusion complexes and physical mixtures were analyzed by scanning electron microscope (JSM 6100 JEOL, Japan). The samples were mounted onto stubs using double sided adhesive tape. The formulations were then coated with gold palladium alloy (150–200Å) using fine coat ion sputter (JEOL, fine coat ion sputter JFC–1100).

The powder X–ray diffraction patterns for all samples were recorded using X–ray diffractometer (Philips PW 1729 X–ray generator computer 1710) operated at voltage 35 kV and a current of 20 mA. The samples were analyzed under conditions: target Cu; filter Ni; receiving slit 0.2 inches; x-axis 10 mm: 1° 2θ; y-axis 2000 cps using Ni filtered Cu-Kα radiation as a source.

The IR spectra of the pure components, the inclusion complexes and the physical mixtures were obtained on (60 MHz Varian EM 360) Perkin Elmer

FTIR spectrophotometer (Perkin Elmer, Switzerland) using the KBr disk technique. The scanning range was 4500–400 cm⁻¹.

Drug content determination

Five mg of the formed complex from each batch was dissolved in 20 mL of methanol/water (1:1) mixture. The drug content was assayed at 278 nm using UV-Visible spectrophotometer (Shimadzu-1601, USA). Each determination was done in triplicate. Percent drug content was calculated for each sample using equation (2).

$$\% \text{ Drug content} = \frac{\text{Measured drug in complex}}{\text{Amount of complex taken}} \times 100 \quad (2)$$

In-vitro release profile studies

The dissolution studies were performed in USP dissolution test apparatus 2 (rotating paddle type). Accurately weighed complexes equivalent to 5 mg of CXB were spread over 900 mL of dissolution medium (phosphate buffer pH 7.4 containing 0.5% SLS). The stirring speed employed was 50 rpm and the temperature was maintained at 37 ± 0.5°C and 10 mL aliquots of dissolution media were withdrawn at various time intervals and replaced by 10 mL of fresh dissolution media. The collected samples were analyzed spectrophotometrically. All assays were run in triplicate.
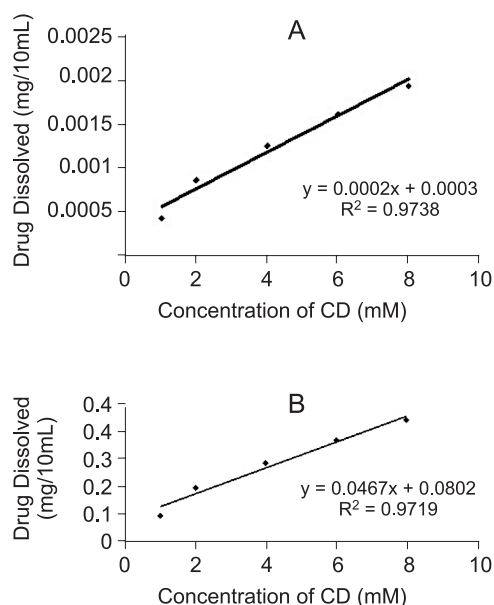
RESULTS AND DISCUSSION

Phase solubility analysis of CXB-HP-β-CD complexes

The solubility of CXB increased in a linear fashion as a function of HP-β–CD concentration which exhibited a typical A_L-type solubility curve (Fig. 1). The apparent stability constants of the inclusion complexes at 25°C and 37°C were found to be 747 M⁻¹ and 601 M⁻¹. The stability constant decreased with increasing temperature probably due to a decrease in the interaction forces, such as van

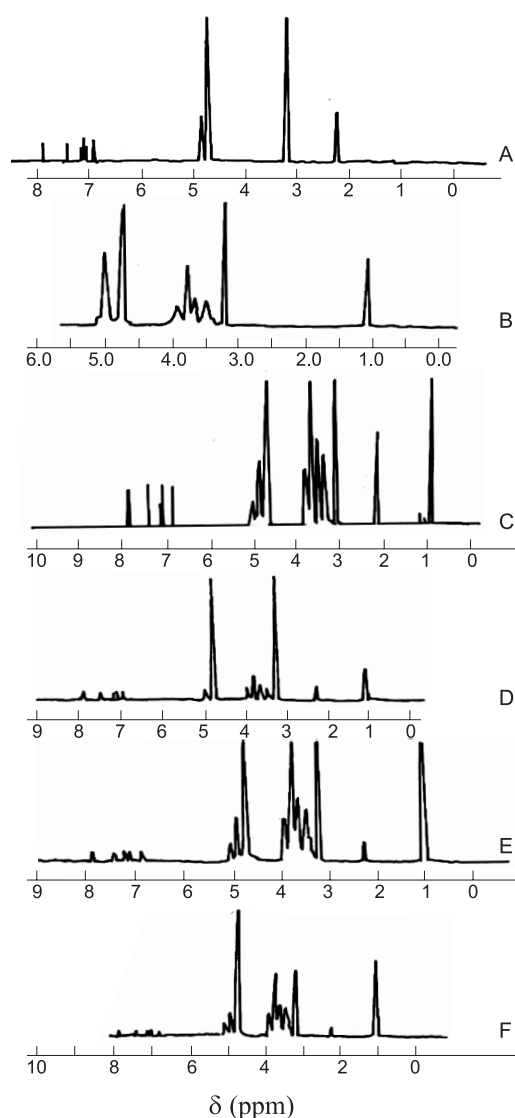Figure 1. a) Phase solubility diagram of CXB: HP-β-CD in water at 37°C (n = 3); b) CXB: HP-β-CD in water at 25°C (n = 3)

Figure 2. NMR spectra A) CXB B) HP-β-CD C) CXBPM1 D) CXBPM2 E) CXBKDHP1 F) CXBKDHP2
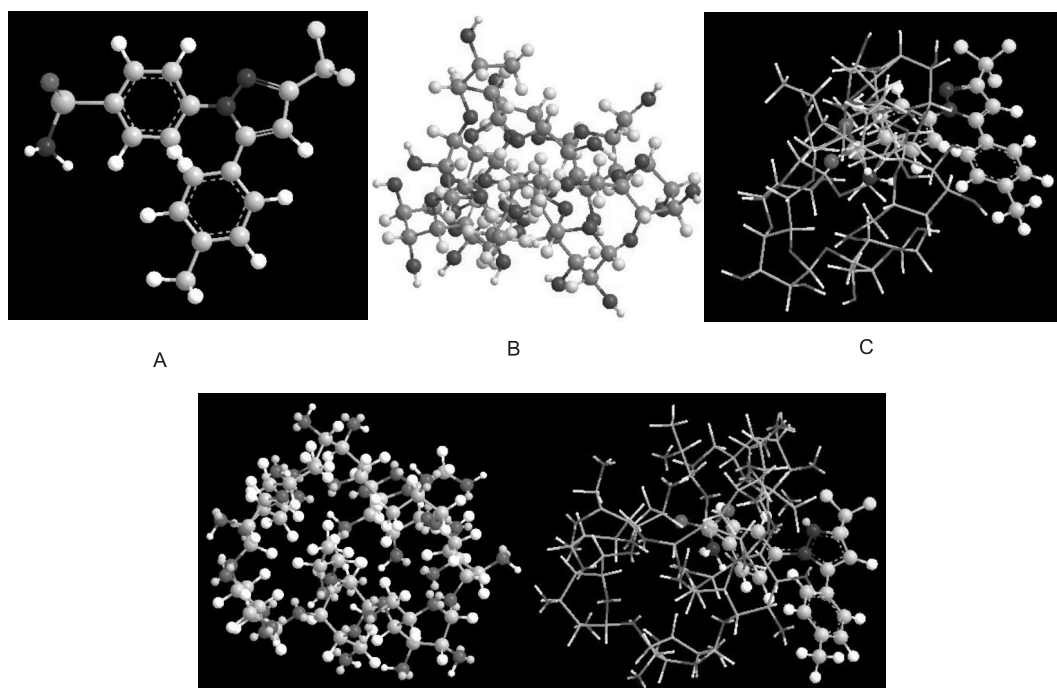
Figure 3. 3D model predictions of the inclusion complex and the minimized energy state forms A) celecoxib CXB; B) HP-β-CD moiety; C) CXB-HP-β-CD complex; D) minimized energy form of HP-β-CD moiety; E) minimized energy form CXB-HP-β-CD complex

der Waals interaction energy and hydrophobic forces between guest molecule and HP-β-CD. In order to determine the thermodynamic parameters (such as Gibbs free energy, ΔG, values obtained at 25°C and 37°C were –4391.3 J/mol and –4723.4 J/mol, respectively) associated with the complexation process, ΔH was calculated from the slope of the plot of solubility *vs.* temperature (van't Hoff equation). The negative enthalpy (ΔH) indicates that the complexation reaction was exothermic (–3855.58 J/mol at 25°C), which was associated with the release of energy that favored formation of the complex. Also, the entropy change was found to be negative (–27.67 J/mol K at 25°C and –28.78 J/mol K at 37°C, respectively) which indicates that complexation of CXB with HP-β-CD resulted in an increase in the order of the system.

NMR spectral analysis

Molecular simulations between the protons resulted into modification of NMR frequencies of both guest (CXB) and host (HP-β-CD) which was physicochemically characterized by ^{1}H-NMR (Fig. 3). Major changes in chemical shift values were observed in the NMR of HP-β-CD region (δ 3.5–3.8), which gives the information about inclusion of guest molecule. In case of physical mixture, CXBPM1 and CXBPM2, there was no change in HP-β-CD protons (Fig. 2C and 2D). The observed signals were sharp, distinct and similar to free CXB spectra (Fig. 2A) and free HP-β-CD (Fig. 2B) spectra, respectively. There was also no change in position of CXB protons signal as well as multiplicity. The splitting pattern of CXB and HP-β-CD did not show any change in case of physical mixtures CXBPM1 and CXBPM2.

The downfield shifts for kneaded complexes CXBKDHP1 and CXBKDHP2 (Fig. 2E and 2F) were in the range of –0.0078 to 0.0346 ppm. The change of H-2 proton of HP-β-CD in kneaded complexes could not be determined because of overlapping with other signals. The H-1 and H-4 protons of HP-β-CD had undergone downfield shift in the signal, which may be not only due to some conformational changes of primary -OH group, but also due to the change in polarity induced by the inclusion of CXB. The H-3 and H-5 protons of HP-β-CD have observed upfield shift in the kneaded complexes, which suggests that these protons are located near the π-electron cloud of an aromatic nucleus and due to its magnetic anisotropy an upfield shift occurs. These results indicated that CXB was embedded in the cavity of HP-β-CD.

The chemical shifts for kneaded complexes were in the range of –0.0061 to 0.0334 ppm. The major changes in the shift position were observed for aromatic protons H-5b, H-1b and H-1a, H-5a protons in the kneaded complexes. The H-4 aromatic protons have observed a slight upfield shift, which suggests that H-4 is near an electronegative group in the cavity. Chemical shifts observed with 5a, 5b protons suggest the possible interaction of p-tolyl part of CXB with the hydrophobic cavity. A possible molecular arrangement for the inclusion compound was that molecule CXB enters the cavity through p-tolyl ring. Insertion of another aromatic ring (sulfamoyl group) in the cavity is ruled out because of its hydrophilic nature. Similar geometry is observed both in CXBKDHP1 and CXBKDHP2 complexes. Further, the 3D model prediction of the inclusion complexes (showing the insertion of p-tolyl part of CXB in HP-β-CD molecule) and its minimized energy state forms as compared to pure drug or HP-β-CD has been illustrated (Fig. 3A- 3E).

Differential scanning calorimetery

DSC thermograms of pure CXB exhibited a sharp endothermic peak at 161.30°C (Fig. 4A). Thermogram of HP-β-CD showed a very broad endothermic peak in the range of 90.03°C (Fig. 4B) due to elimination of water of crystallization as reported by many authors (13). The endothermic peak of the drug was retained at 159.67°C in physical mixture CXBPM1, while a broad peak corresponding to HP-β-CD appeared in the range of 84.70°C in case of physical mixture (Fig. 4C). These observations may be attributed to the presence of weak or no interaction between the pure components in the physical mixture.

DSC thermogram of CXBKDHP1 displayed an endothermic peak at 62.05°C (Fig. 4D) while endothermic peak of CXB which appeared at 159.67°C in case of the physical mixture was absent in the thermogram of the complex. Hence, it may be ascribed to the formation of inclusion in case of kneaded complexes (14, 15).

Scanning electron microscopy

The scanning electron microphotographs of CXB-HP-β-CD inclusion complex and their physical mixture are shown in Fig. 5. CXB appeared as needle-shaped crystals (Fig. 5A) and HP-β-CD (Fig. 5B) exhibit somewhat spherical shape. The physical mixture retained the characteristics of both CXB (crystalline nature) and HP-β-CD (amorphous nature). The SEM of kneaded complexes (Fig. 5D

and 5E) showed a drastic change in the shape and morphological features. The physical mixture showed the crystalline structure of CXB and HP-β-CD, which revealed that apparently no interaction has taken place in the solid state (Fig. 5C).

X-ray diffraction analysis

The powder X–ray diffraction patterns of pure CXB, HP-β-CD, their physical mixtures and inclusion complexes are represented in Figure 6. HP-β-CD (Fig. 6B) exhibited no sharp peaks due to its amorphous nature. Most of the principal peaks of CXB and HP-β-CD were present in the diffraction patterns of physical mixtures indicating low interaction between the pure components in case of physical mixtures (Fig. 6C).
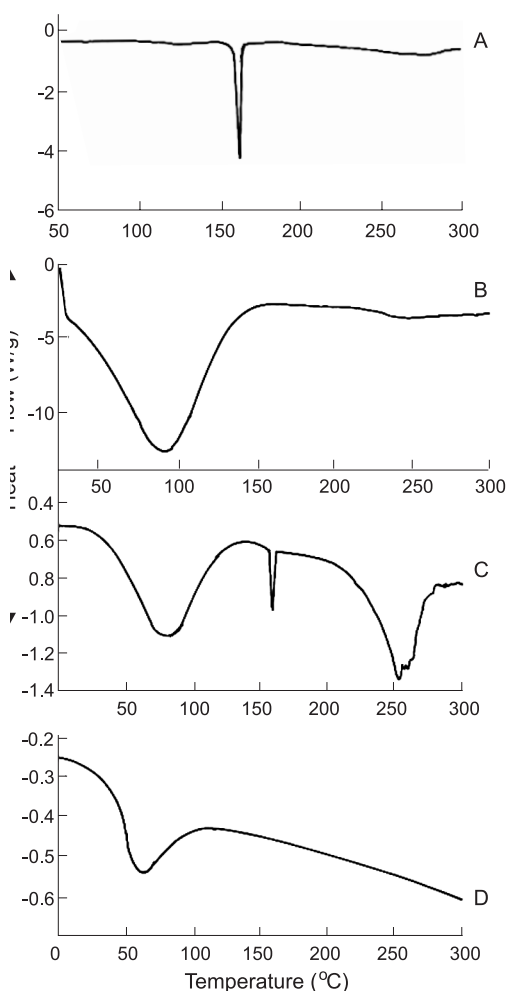

Figure 4. DSC analysis: A) CXB; B) HP-β-CD; C) CXBPM1; D) CXBKDHP1
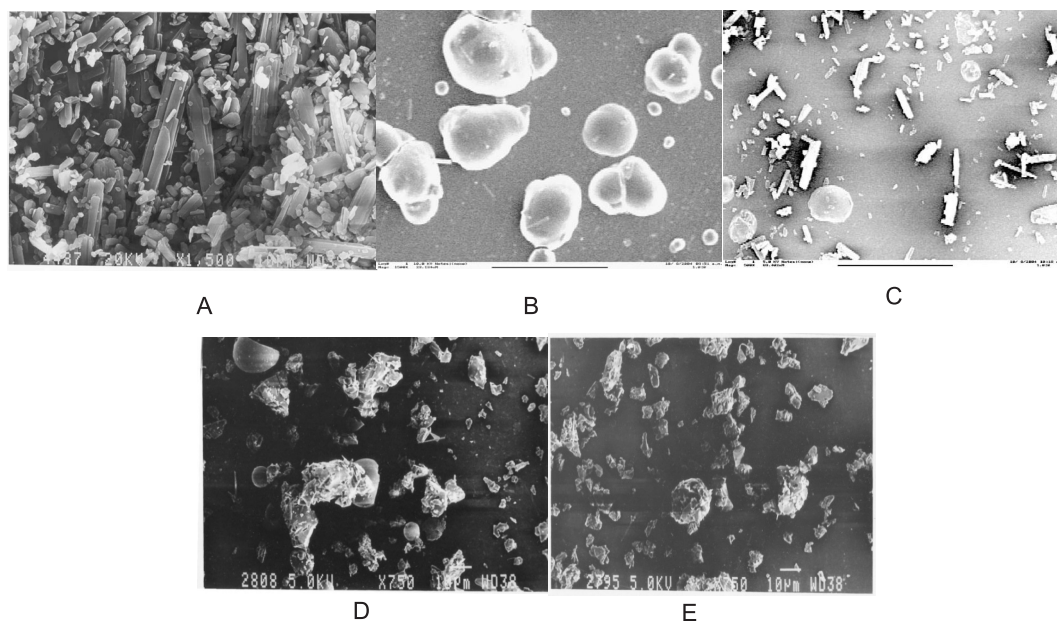
Figure 5. SEM photographic analysis of A) CXB; B) HP-β-CD; C) CXBPM1; D) CXBKDHP1; E) CXBKDHP2

However in contrast, kneaded complexes (CXBKDHP1 and CXBKDHP2) showed disappearance of major peaks corresponding to both CXB and HP-β-CD (Fig. 6D and 6E). Many peaks of pure CXB were not present and the formed products were amorphous in nature, which is indicative of existence of inclusion complex (16). The diffraction pattern was more towards the pure HP-β-CD. Only few peaks were observed and they too were quite different from the one observed with pure CXB confirming the formation of complex.

FTIR spectroscopy

IR spectrum of CXB (Fig. 7A) showed medium absorption bands at 3340 and 3234 cm^{-1} that were assigned to drug –NH symmetric and asymmetric stretching vibrations. The other characteristic bands may be attributed to the following group vibrations: 1163.6 cm^{-1} and 1348 cm^{-1} (S=O symmetric and asymmetric stretching, respectively) and 793.4 cm^{-1} (aromatic CH bending). The IR spectrum of HP-β-CD (Fig. 7B) showed a broad absorption band at 3395.9 cm^{-1} due to –OH stretching.

Broad peak at 3392.6 cm^{-1} indicated the masking of characteristic –NH stretching bands of symmetric at 3234.5 cm^{-1} and asymmetric at 3340.5 cm^{-1}. These observations led to the conclusion that there might be some interaction between CXB and β-CD in the physical mixture (Fig. 7C).

A single broad peak at 3392.5 cm^{-1} indicated the masking of characterstic symmetric and asymmetric stretch in case of 1:1 kneaded complex (CXBKDHP1) and at 3396.9 cm^{-1} in case of 1:2 kneaded complex (CXBKDHP2) (Fig. 7D and 7E). This is attributed to the intermolecular hydrogen bonds of the crystals and formation of a monomeric dispersion of a drug as a consequence of the interaction with HP-β-CD which could result from the inclusion of the drug in the hydrophobic cavity. The S=O band at 1348.0 cm^{-1} became broadened and appeared at 1347.5 cm^{-1} (CXBKDHP1) in the kneaded complexes. Also, the sharp C-F bending vibration at 1163.6 cm^{-1} due to CF$_3$ became broadened in the kneaded complexes. The broadening of S=O stretching at 1348.0 cm^{-1}, CF stretching at 1163.6 cm^{-1} and masking of NH stretching bands in kneaded complexes signify the existence of some interaction between the drug and HP-β-CD.

***In-vitro* release studies**

The *in-vitro* dissolution profile of pure drug showed only < 30% release of the drug even after 30 min and 42.07% in 90 min, respectively (Fig. 8). The physical mixtures CXBPM1 and CXBPM2 showed slightly higher amount of drug release at each sampling interval as compared with dissolution profile of pure drug.

Batches CXBKDHP1 and CXBKDHP2 displayed better dissolution profile as compared to the
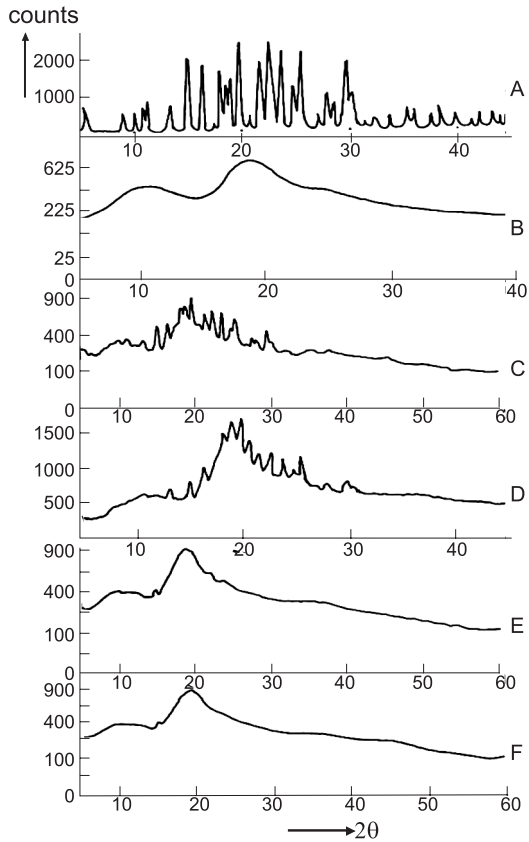
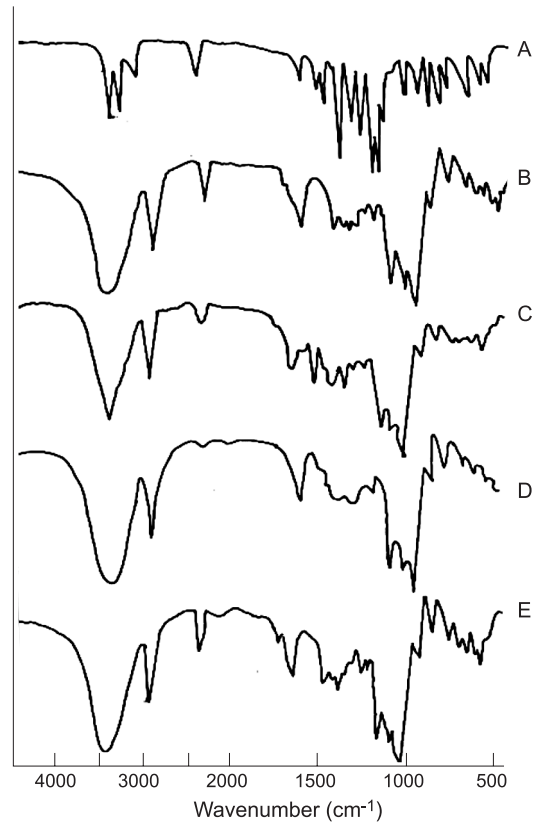Figure 6. X-ray diffraction pattern of A) CXB; B) HP-β-CD; C) CXBPM1; D) CXBPM2; E) CXBKDHP1; F) CXBKDHP1

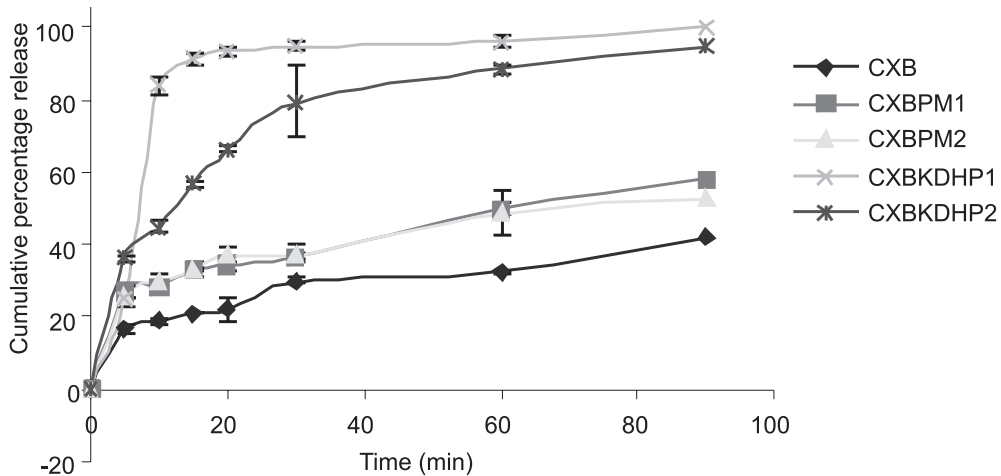Figure 7. FTIR analysis A) CXB; B) HP-β-CD; C) CXBPM1; D) CXBKDHP1; E) CXBKDHP1

Figure 8. Dissolution profiles of pure CXB, CXBPM1, CXBPM2, CXBKDHP1, CXBKDHP2 (mean ± SD, n = 3)

pure drug and physical mixtures, as depicted in Fig. 8. An enhanced rate and extent of drug release was obtained at each time intervals. CXBKDHP1 released about 83.73% of the drug in 10 min, where-as CXBKDHP2 showed about 44.88% drug release in the same time. Complete drug release was obtained from kneaded complex CXBKDHP1 and over 94.62% drug was released from complex

CXBKDHP2 in the same time. Thus, it can be inferred that CXBKDHP1 demonstrated higher enhancement of dissolution compared to CXBKDHP2. The significant improvement in dissolution characteristics of the complexes was justified through the concurrence of several factors: increased particle wettability, reduction of crystallinity of the product and simultaneously interfacial tension between the solid particles of CXB or the dissolution medium (17, 18).

The mean percent release of drug from kneaded complexes CXBKDHP1 and CXBKDHP2 at 30 min was 3.18 and 2.66 fold higher with respect to pure CXB. The physical mixtures CXBPM1 and CXBPM2 also increased the mean percent release of drug by 1.23 and 1.25 fold, respectively.

CONCLUSION

The study concludes that CXB was entrapped into HP-β-CD, forming an inclusion complex in both ratios (1:1, 1:2) The physicochemical interpretation of the data (through NMR, DSC, SEM, XRD, FTIR) revealed the confirmation of molecular simulation of the atoms of CXB and HP-β-CD, which led to penetration of hydrophobic COX-II inhibitor into the cavity. The 1:1 kneaded complexes showed better dissolution rate and solubility as compared to 1:2 complexes. This will further help in reducing the dose of NSAIDs due to better absorption and higher COX-II activity in the pharmaceutical dosage forms for the chemoprevention of cancer.

REFERENCES

1. Szejtli J.: Pure Appl. Chem. 76, 1825 (2004).
2. Thompson D.O.: Crit. Rev. Ther. Drug Carr. Syst. 14, 1 (1997).
3. Irie E., Uekama K.: J. Pharm. Sci. 86, 147 (1997).
4. Sinha V.R., Bindra S., Kumria R., Nanda A.: Pharm. Technol. 22, 120 (2003).
5. Challa R., Ahuja A., Ali J., Khar R.K.: AAPS PharmSciTech. 6, E329 (2005).
6. Brewster M.E., Loftsson T., Estes K.S., Lin J.L., Frioriksdottir, H.: Int. J. Pharm. 79, 289 (1992).
7. Ramos Rocha, F.T., Lourenço L.G., Jucá M.J., Costa V., Leal A.T.: Acta Cir. Bras. 24, 189 (2009).
8. Maier T.J., Schilling K., Schmidt R., Geisslinger G., Grosch S.: Biochem. Pharmacol. 67, 1469 (2004).
9. Tae J.J., Ho G.J., Ki H.J., Min K.: Int. J. Exp. Pathol. 83, 173 (2002).
10. Paulson S.K., Vaughn M.B., Jessen S.M., Lawal Y., Gresk C.J., Yan B., Maziasz T., Cook C.S., Karim A.: J. Pharmacol. Exp. Ther. 297, 638 (2001).
11. Higuchi T., Connors A.K.: Phase-solubility techniques. In: Advances in Analytical Chemistry and Instrumentation. Reill CN (Ed.), pp. 117–212, John Wiley & Sons, New York 1965.
12. Ashwinkumar C.J., Moji C.A.: Int. J. Pharm. 212, 177 (2001).
13. Veiga M.D., Diaz P.J., Ahsan F.: J. Pharm. Sci. 55, 891 (1998).
14. Mura P., Faucci M.T., Parrini P.L., Furlanetto S., Pinzauti S.: Int. J. Pharm. 179, 117 (1999).
15. Mura P., Adragna E., Rabasc A.M., Moyano J.R., Perez-Martinez J.I., Arias M.J., Gines J.M.: Drug Dev. Ind. Pharm. 25, 279 (1999).
16. Sinha V.R., Anitha R., Ghosh S., Nanda A., Kumria R.: J. Pharm. Sci. 94, 676 (2005).
17. Becirevic-Lacan M., Filipovic-Grcic J., Skalko N., Jalsenjak J.: Drug Dev. Ind. Pharm. 22, 1213 (1996).
18. Moyano J.R., Arias Blanco M.J.A., Gines J.M., Perez-Martinez J.I., Rabasco A.M.: Drug Dev. Ind. Pharm. 23, 379 (1997).